HHS Public Access

Author manuscript

Hepatology. Author manuscript; available in PMC 2018 October 01.

Published in final edited form as:

Hepatology. 2017 October ; 66(4): 1258–1274. doi:10.1002/hep.29276.

Loss of L- Selectin Guided CD8+ but not CD4+ Cells, Protects Against Ischemia Reperfusion Injury in a Steatotic Liver

Vasantha L. Kolachala[1], **Sirish Palle**[1], **Ming Shen**[1], **Alayna Feng**[1], **Dmitry Shayakhmetov**[1], and **Nitika A. Gupta**[1,2]

[1]Department of Pediatrics, Emory University School of Medicine, Atlanta, GA

[2]Transplant services, Children's Healthcare of Atlanta. Atlanta, GA

Abstract

Background & Aims—Steatotic liver responds with increased hepatocellular injury when exposed to an ischemic-reperfusion insult. Increasing evidence supports the role of immune cells as key mediators of this injury in a normal (lean) state, but data about their role in a steatotic liver are practically non-existent. The objective of the current study was to delineate contribution of specific phenotypes of T cells and adhesion molecules in exacerbated cell death in steatotic liver injury.

Methods—RNA sequencing was performed on isolated steatotic primary hepatocytes and T cell markers were assessed in hepatic lymphocytes after ischemia reperfusion injury (IRI) in high fat diet (HFD) fed mice. $CD8^{-/-}$ and $CD4^{-/-}$ mice along with CD8 and L-selectin antibody treated mice were fed on a HFD and hepatocellular injury was assessed by histology, propidium iodide injection and ALT after IRI.

Results—RNA sequencing demonstrated a strikingly differential gene profile in steatotic hepatocytes vs. lean hepatocytes. After injury, the HFD liver showed increased necrosis, infiltrating $CD8^+$ cells, ALT and proinflammatory cytokines. Hepatic lymphocytes demonstrated increased $CD8^+/CD62L^+$(L-selectin) cells in HFD fed mice after IRI. $CD8^{-/-}$ mice and CD8 depleted C57BL/6 mice, demonstrated significant protection from injury, which was not seen in $CD4^{-/-}$ mice. L-selectin blockade also demonstrated significant hepatoprotection from IRI. L selectin ligand MECA-79 was increased in HFD fed mice undergoing IRI.

Conclusion—Blockade of CD8 and L-selectin but not CD4, ameliorated hepatocellular injury, confirming that $CD8^+$ cells are critical drivers of injury in a steatotic liver. This represents a novel therapeutic target in steatotic liver injury, underlining the importance of development of therapies specific to a steatotic liver.

Keywords

mouse model; NAFLD; steatosis; liver damage; adhesion molecules; MECA-79; L-selectin; $CD8^+$

Corresponding Author: Nitika Arora Gupta, MD, DCH, DNB, MRCPCH, Associate Professor of Pediatrics, 1760 Haygood Drive, Atlanta, GA 30322, Phone: 404-727-2026; Facsimile: 404-727-4069, nitika.gupta@emory.edu.

Conflict of Interest Statement:

The authors declare that they have no conflicts of interest relevant to this work

Introduction

The proportion of obese adults in the United States has greatly increased since the 1960s, from 13.4% to 35.7%; it has been estimated that more than two thirds of adults are overweight or obese (1–3). Non-alcoholic fatty liver disease (NAFLD) is a sequel of obesity with a range of clinical severity from benign steatosis to severe steatohepatitis, and then potentially fatal end-stage liver disease that requires liver transplantation (4, 5). Ischemia reperfusion injury (IRI) in the liver occurs during shock, myocardial infarction, following hepatectomy, and liver transplantation. A fatty liver is increasingly susceptible to IRI and develops increased hepatocellular dysfunction and cell death compared with a non-fatty liver. When exposed to IRI, patients with NAFLD develop extensive liver injury leading to long hospital stays and increased morbidity and mortality. NAFLD is expected to surpass hepatitis C as the most common indication for liver transplantation by 2030 (6). With wait lists for liver transplant increasing, there has been a decrease in availability of healthy donor organs, because significant proportions of donor livers are fatty, and hence unsuitable for transplantation. Measures to reduce cell injury and death in fatty livers exposed to IRI could increase the number of organs available for transplantation. The mechanisms by which hepatocytes undergo cell death in the fatty liver after IRI have not been sufficiently explored. We have shown that a fatty liver, compared with a lean liver, has increased necrosis, apoptosis and autophagy after IRI (7, 8), which is associated with progression to fibrosis, cirrhosis and hepatocellular carcinoma. Several groups have shown that $CD4^+$ cells are the main drivers of IRI in a lean state (9–11), but the role of lymphocytes in IRI of NAFLD is virtually unknown. Interestingly, there is an increase in lymphocyte trafficking across endothelial cells in NAFLD (12), suggesting that these cells may contribute to the exacerbated tissue response to injury after IRI.

Proteins in the selectin family mediate leukocyte migration and recruitment (13, 14). L-selectin (also known as CD62L) is a lymphocyte-homing receptor, expressed by most leukocytes (15). It is an important mediator of inflammation, which is expressed on $CD4^+$ and $CD8^+$ cells, and is involved in pathogenesis of several different disorders (16–19), including IRI in the lean liver (20–23).

It has not been clear whether there is a role for L-selectin in the response of the fatty liver to IRI. We investigated the role of L-selectin–induced lymphocyte recruitment as an underlying mechanism of hepatocellular damage in fatty livers using a mouse model of IRI.

Methods

ANIMALS

The Institutional Animal Care and Use Committee (IACUC) of Emory University approved all procedures performed on animals. Mice were maintained on a 12-hour dark-light cycle and allowed free access to food and water under conditions of controlled temperature (25±2°C).

DIETS

C57BL/6, CD8$^{-/-}$, CD4$^{-/-}$ male mice were obtained from Jackson Research Laboratories at 4 weeks of age. Mice were divided into groups given a regular mouse chow or a high fat diet (HFD) (60% fat; Research Diets Inc., NJ) *ad libitum* for 12 weeks before IRI. Body weights were monitored at regular intervals. Livers were collected and steatosis was confirmed by Oil red O staining on frozen sections.

TISSUE TRIGLYCERIDE QUANTIFICATION

Triglycerides were quantified in liver tissues by Triglyceride assay according to manufacturer's instructions and were expressed as nmol/mg liver tissue.

ISCHEMIA REPERFUSION INJURY

Wild type C57BL/6 mice fed a HFD were divided into 4 subgroups of 10 mice each: no IRI (control), IRI+, IRI with injection of a CD8-depleting antibody, or IRI with injection of anti-mouse CD62L (anti L-selectin antibody). An equivalent number of mice fed normal chow were used as lean controls. Similar studies were also performed with CD8$^{-/-}$ and CD4$^{-/-}$ mice fed a HFD. Animals were anesthetized with pentobarbital (50 mg/kg) and IRI was induced as previously described (7). A clamp was placed on the portal vein and the hepatic artery blocking blood flow to the left and medial lobes of the liver, inducing partial hepatic ischemia. The clamp was removed after 40 minutes to allow reperfusion. The mice were sacrificed after 24 hours of reperfusion, and liver tissue and blood samples were collected. Sham surgeries were also performed along with controls for all the experiments.

PRIMARY HEPATOCYTE ISOLATION

At the time of sacrifice, the livers were perfused with liberase enzyme (10 units) to separate parenchymal and non-parenchymal cells. Hepatocytes were purified using a percoll gradient.

RNA SEQUENCING

Purified hepatocytes from lean and HFD-fed mice were analyzed for their genome-wide transcriptional profiles using a next-generation RNA- sequencing approach at Integrated Emory University Genomics Core. Genes were grouped into functionally related genes using DAVID functional annotation tool, and heat maps were generated using R programming.

HISTOLOGY

Paraffin sections of the entire ischemic lobe of the liver of lean and HFD fed mice undergoing IRI were stained with hematoxylin and eosin (H&E). The sections were scanned using a bright-field scanner (Hamamatsu Nano zoomer 2.0 H) in the Department of Pathology, Emory University. Aperio image scope software (Leica Biosystems Imaging Inc.) was used for assessment of total necrotic area and nuclear count per high power field. Scanned, high-resolution images were used to outline the necrotic area (white line) and nuclear counting was performed using the algorithm provided in the software. Based on recommendations of the nomenclature committee on cell death (24) we also calculated a manual, detailed morphologic score using selective histological criteria for necrosis as shown in Table 1.

HEPATOCELLULAR INJURY

Hepatocellular injury was assessed *in vivo* by measuring serum levels of alanine aminotransferase (ALT) in the Division of Animal Resources, Emory University. To assess cell death due to cell membrane permeability, mice were given intravenous injections of propidium iodide (Sigma Aldrich) 10 minutes before sacrifice. Frozen sections were cut and red fluorescent intensity was captured by fluorescent microscopy (Olympus) and quantified using Fiji software.

LUMINEX ASSAY

Levels of cytokines in serum samples of lean and HFD-fed mice were determined using the mouse Luminex Bead Cytokine 20-plex Kit (Invitrogen) according to the manufacturer's protocol.

HEPATIC LYMPHOCYTE ISOLATION

Liver tissues were minced and placed in RPMI media with 10% FBS. Cells were centrifuged @ 300 g for 5 min to discard hepatocytes. Then the pellet was re-suspended in 40% percoll, topped over 60% percoll solution and centrifuged at 2000 rpm x 20 minutes. Hepatocytes were in the surface layer and lymphocytes were collected from the interface. The lymphocyte fraction was re-suspended in RPMI and centrifuged at 1500 rpm for 5 minutes. The single-cell suspension was checked for viability and stained for CD3, CD4, and CD8, and CD62L (L-selectin).

IMMUNOFLUORESCENCE

Frozen liver tissue sections from all groups were fixed, blocked and incubated with primary antibody CD8, CD34, CD62L (Abcam, MA) and MECA-79 (Biolegend, CA). Then the tissues were probed with secondary antibodies and counter stained with nuclear stain DAPI. Images were taken using Olympus FV1000 confocal laser-scanning microscope (Olympus America Inc.) and the generated data sets were analyzed using Imaris 8.4 (Bitplane) for 3D co-localization and visual overlap at Emory Integrated Cellular imaging Core.

IMMUNOHISTOCHEMISTRY

Liver tissue sections were deparaffinized and antigens were retrieved. They were exposed to H_2O_2 to quench endogenous peroxidase. Tissues were blocked and incubated with an anti - CD3 antibody, anti-rabbit secondary antibody and then with Diamino benzidine substrate. After counter staining with hematoxylin, the tissue sections were visualized under a light microscope.

FLOW CYTOMETRY

One million hepatic lymphocytes were washed, incubated with an Fc receptor blocker and then with antibodies against CD3, CD4, or CD8 at 4^1C. A live/dead cell kit was used (Bio legend). Cells were compensated with ArC-reactive and ArC-negative beads (Molecular Probes) and analyzed on a Becton-Dickenson flow cytometer (LSR II) at the Emory Children's Pediatric Flow Cytometry Core.

REAL-TIME PCR

Total RNA was extracted from livers of lean mice and HFD fed mice, with and without IRI. Liver tissues were homogenized and RNA was extracted using an RNAeasy Minikit (Qiagen). cDNA was made using the high-capacity cDNA reverse transcription kit (Applied Bio systems). The sequences of the primers used for RTPCR for P, E and L-selectin are listed in Table 2.

BLOCKADE OF L-SELECTIN

A functional grade purified antibody for anti-mouse CD62L (anti L-selectin) was obtained from eBiosciences (clone MEL-14). Two doses of 100 μg each were given intravenously to lean and HFD fed mice on day -1 and the day 0 (day of IRI). Rat IgG2a isotype control was used in similar doses (eBiosciences).

$CD8^+$ DEPLETION

Before IRI, mice fed a HFD were given 3 intra peritoneal injections (400 ug each) of CD8 antibody (clone 53–6.72, BioXcell) on day-2, day-1 and on the day of IRI. A rat monoclonal antibody against (IgG2a) was used as a negative control.

STATISTICAL ANALYSES

Groups were compared using Student *t* test for two groups, one-way ANOVA for three or more groups and Two-way Anova for four or more groups (GraphPad Prism 6). A probability value of $p<0.05$ was considered significant.

RESULTS

HIGH FAT DIET FED MICE HAVE INCREASED HEPATOCELLULAR INJURY AND NUMBER OF INTRAHEPATIC $CD3^+$ T CELLS AFTER IRI

Mice were fed a HFD diet for 12 weeks and their weight gain measurements, liver fat accumulation and liver triglyceride content is shown in supplemental figure 1A-D. Additionally, differential gene expression analysis by RNA sequencing of isolated primary lean and steatotic hepatocytes is shown in supplemental Figure 1E. To further explore the immune response, after Ischemia reperfusion injury we assessed the frequency of $CD3^+$ cells in the liver after IRI by immunohistochemistry (IHC). Livers of lean and HFD mice showed no difference in numbers of $CD3^+$ cells (Figure 1A, top panel) at baseline. After IRI, $CD3^+$ cells were significantly increased in livers of mice with steatosis (Figure 1A, bottom panel). Quantification for $CD3^+$ cells is shown in Figure 1B ($p<0.0004$).

To confirm our IHC findings we did flow cytometry analysis of total liver lymphocytes. At baseline, lean and HFD fed mice showed no difference in $CD3^+$ cells (30.2±1.1% vs. 32.5±1.5%; Figure 1C, top panel; Figure 1D). On the other hand, mice fed a HFD subjected to IRI had significantly more $CD3^+$ cells in the liver (44.8±2.4%) compared to lean mice (32.4±0.1% $p<0.0001$, Figure 1C, bottom panel; Figure 1D), confirming IHC findings. Thus, IRI in fatty liver not only increases necrosis as shown in our earlier studies (7, 8) but also leads to increased infiltration of $CD3^+$ cells, as compared to the lean liver undergoing IRI.

INCREASED SERUM LEVELS OF PRO-INFLAMMATORY CYTOKINES IN HFD FED MICE AFTER IRI

We analyzed levels of proinflammatory cytokines in serum samples from lean and HFD fed mice, with and without IRI. Serum from mice fed a HFD had significantly higher levels of pro-inflammatory cytokines compared to lean mice after IRI or mice on a HFD without IRI (Figure 2). Levels of IL-6 were 10.5±0.5 pg/ml in lean mice undergoing IRI, and 24.1±4.4 pg/ml in mice on a HFD undergoing IRI ($p<0.0004$) IL-1β: lean IRI+ 7±0.2 vs. HFD IRI + 15.0±3.6 pg/ml ($p<0.005$,) keratinocyte-derived chemoattractant (KC): lean IRI+ 123±30 vs. HFD IRI+ 970±372 pg/ml ($p<0.0001$); IL-2: lean IRI+18±1.6 vs. HFD/ IRI+ 135±64 ($p<0.0001$); IFNγ-induced protein (IP10): lean IRI+ 20±0.5 vs. HFD IRI+ 40±4.9 pg/ml ($p<0.0009$); monokine induced by IFNγ (MIG): lean IRI+ 14±1.2 vs. HFD IRI+ 564±324.6 pg/ml ($p<0.0001$). These findings indicate that imposing IRI on steatotic liver increases systemic production of proinflammatory cytokines.

LOSS OF $CD8^+$ BUT NOT $CD4^+$ CELLS, PROTECTS AGAINST ISCHEMIA REPERFUSION INJURY IN HFD FED MICE

Since the livers of HFD fed mice contain more $CD3^+$ cells than lean livers after IRI, we investigated the role of $CD3^+$ subsets as potential mediators of increased liver injury. We compared liver injury after HFD and IRI in C57BL/6, $CD4^{-/-}$, and $CD8^{-/-}$ mice, and CD8 antibody depleted mice.

Compared to WT mice, $CD8^{-/-}$ mice on HFD exposed to IRI exhibited significantly less necrosis as outlined by white lines in H&E images (Figure 3A). Necrosis was further quantified by Aperio software as described in Methods. $CD8^{-/-}$ mice showed more intact nuclei compared to WT (136 vs. 38 ± 9/field; $p<0.0001$) along with a substantially decreased necrotic area ($4.2x10^6$ vs. $3.5x10^7$; $p<0.002$). Calculated necrosis score was also significantly lower (11.6 vs. 25.1±3.9; $p<0.01$). Serum ALT levels were significantly lower in $CD8^{-/-}$ mice (326 vs. 986 IU/l; $p<0.04$) corroborating the histological findings. There was no statistical difference in necrotic changes between WT and $CD4^{-/-}$ either histologically or biochemically. The body weight changes (Suppl. Figure 2) between $CD4^{-/-}$ and $CD8^{-/-}$ mice fed a HFD were similar. These results suggest that $CD8^+$ cells but not $CD4^+$ cells play a critical role in the IRI mediated liver cell injury in steatotic liver. To further corroborate the data from KO mice we depleted $CD8^+$ cells using anti-CD8 specific antibody and determined whether such depletion conferred protection from IRI in steatotic liver. C57BL/6 WT mice were given either the anti-CD8 depleting antibody (under conditions that depleted >90% of $CD8^+$ cells; Suppl. Figure 3), or the control IgG. Compared to mice receiving control IgG, mice receiving a CD8 depleting antibody exhibited decreased necrosis histologically (Figure 3D), significantly more intact nuclei (83±6 vs. 41±5; $p<0.0001$), lesser necrotic area ($2.8x10^6$ vs. $4.1x10^7$; $p<0.001$), lower calculated necrosis score (5.7±1.4 vs. 19.2±3.1; $p<0.0002$) and lower serum ALT (657±103.8 vs. 1536±294 IU/L; $p<0.05$) corroborating the findings in $CD8^{-/-}$ mice.

These findings clearly support the suggestion that $CD8^+$ cells are important mediators of IRI induced injury in a steatotic liver.

CD8$^+$ CELLS MEDIATE ISCHEMIA REPERFUSION INJURY IN HFD FED MICE VIA L-SELECTIN

If CD8$^+$ cells mediate the damage in steatotic liver IRI, their trafficking to the liver is likely mediated by adhesion molecules the genetic signature for which was up regulated in steatotic hepatocytes (Figure 1). Hence we further investigated if the selectin family of the adhesion molecules modulates this process. Analysis of selectin expression in the liver shows that levels of L-selectin mRNA were significantly increased in the liver of HFD fed mice with IRI, compared with lean mice with IRI (2.0±0.2 in HFD mice with IRI vs. 0.83±0.1 fold increase in lean mice with IRI; $p<0.003$) and as compared to HFD liver without IRI (0.25±0.1; $p<0.0003$). In contrast, levels of P- and E-selectin mRNAs were not significantly increased after IRI in HFD fed mice (Figures 4A). Sham treated mice did not show any difference from controls.

Flow cytometry analysis of lymphocytes from livers of mice fed a HFD indicated that CD4$^+$/CD62L$^+$ cells (CD3 gated) were slightly increased with IRI (not significant), whereas CD8$^+$/CD62L$^+$ cells were significantly increased following IRI (Figure 4B, $p<0.0002$).

MECA-79 is a carbohydrate epitope found on a family of sialomucins known as peripheral node addressins that serve as ligands for L-selectin. Immunofluorescence analyses showed that livers of HFD fed mice subjected to IRI had increased expression of MECA-79, which co-localized with endothelial cells (marker CD34). MECA-79 was not detected in livers of lean mice undergoing IRI or HFD fed mice without IRI (Figure 4C,D). Thus, HFD IRI mice showed endothelial cell transformation by expressing MECA-79. This was further confirmed by 3D image analysis and quantification as shown in Figure 4E,F. These observations strongly suggest that L-selectin adhesion molecule with it's ligand MECA-79, leads to the trafficking of CD8$^+$ cells into the liver which contribute to exacerbated liver injury seen in steatotic mice undergoing hepatic IRI.

In order to further evaluate this observation, we blocked L-selectin and assessed if this would independently lead to amelioration of hepatocellular injury in HFD fed mice after IRI.

BLOCKING L-SELECTIN REDUCES HEPATOCELLULAR INJURY IN HFD FED MICE AFTER IRI

Mice were given L-selectin blocking antibody and blockade was confirmed by flow cytometry (Suppl. Figure 4). Livers from HFD fed mice given the L-selectin blocking antibody demonstrated less necrosis after IRI compared with HFD fed mice given the control antibody, as outlined by white lines in H&E images (Figure 5A). L-selectin Ab treated mice showed more intact nuclei compared to control IgG (99±7 vs. 37±5 /field; $p<0.0001$) along with a substantially decreased necrotic area ($2.5x10^6$ vs. $2.7x10^7$; $p<0.005$). Calculated necrosis score was also significantly lower (5.2±2.0 vs. 19.2±3.1, $p<0.002$). Serum ALT levels were significantly lower in L -selectin Ab treated mice (289.9±79.8 vs. 986.5±87.4 IU/L, $p<0.004$) corroborating the histological findings. The decreased liver injury was also confirmed by determining the number of propidium-iodide (PI) positive cells in the liver which showed a remarkable reduction in PI positive cells in HFD fed mice

treated with L-selectin Ab as compared to IgG treated HFD control mice (20.2±0.2 vs. 48.6±4.6 pixels, $p<0.003$; Figure 5D).

Levels of proinflammatory cytokines in serum were also decreased after L-selectin blockade. Mice fed a HFD and given L-selectin antibody with IRI had decreased levels of IL-6 (29.0±6.2 pg/ml), as compared to mice fed HFD but given control IgG (64.4±13.3 pg/ml; $p<0.04$). Similarly, the serum levels of IP-10 in mice on HFD given L-selectin antibody with IRI were low (24.4±2.2 pg/ml) as compared to mice given a control IgG (91.0±2.4 pg/ml $p<0.03$ Figure 5E). Thus blockade of L-selectin adhesion molecule led to decreased hepatocellular injury and lower levels of proinflammatory cytokines in HFD fed mice undergoing IRI.

Figure 6 is a schematic representation of the possible mechanism by which $CD8^+$ cells, guided by L selectin-MECA 79 mediated trafficking, lead to hepatocellular injury in HFD fed mice undergoing IRI.

Discussion

With increasing incidence of NAFLD, it is now being recognized that a steatotic liver when exposed to injury, has a worse clinical outcome (25–34). Dynamics of microcirculation (35–38) and ischemic injury (39) differ in steatotic liver compared to lean liver, implying that our current understanding of host response to injury in a ‘lean or normal’ state does not necessarily apply fully to a steatotic liver. In this study, we show that $CD8^+$ cells are essential for the increased liver damage that occurs in steatotic liver during IRI, compared with lean liver. We observed that $CD8^+$ cells are recruited to the liver by L-selectin, a receptor on the T cells that binds to the ligand MECA-79, seen on endothelial cells of the fatty liver but not in lean liver after IRI. Depletion of $CD8^+$ cells or knockout of CD8 in mice protects the liver from the combined damage of steatosis and IRI, reducing necrosis and serum levels of ALT. We also observed similar protective effects by treating the mice with L-selectin blocking antibody. These novel findings demonstrate for the first time, the role of $CD8^+$ cells as critical regulators of liver damage in a steatotic liver undergoing IRI verses the current understanding of $CD4^+$ cells as being the main drivers of injury based on data from lean settings.

Lymphocytes in general and T lymphocytes in particular, have been implicated in IRI of several organs. It is well known that lymphocytes play more than a bystander role. Thus far, $CD4^+$ cells have been considered to be the key mediators of IRI. Several studies have shown that in IRI of the lung (40), brain (41), myocardium (42), intestine (43), and kidney (44), deficiency of $CD4^+$ cells leads to protection from injury. $CD4^+$ cells have also been similarly implicated in hepatic IRI (9, 45). Zwacka et al., demonstrated the pathogenicity of $CD4^+$ cells by subjecting athymic (nu/nu) mice to hepatic IRI (10) and Khandoga et al. showed improvement in hepatic perfusion in CD4 deficient mice after IRI (46). It is important to note that both these studies were conducted in normal or ‘lean’ mice and not in HFD fed mice as in our study, which is a different functional and activation state. This once again underlines the importance of differential cell types and mechanisms, which are operational in a steatotic liver IRI.

The role of $CD8^+$ cells has not been as well studied in IRI as $CD4^+$ cells. Many studies have been done in $Rag1^{-/-}$ or T cell deficient mice (41, 47), which have combined T cell deficiencies making the exact contribution of the CD4 and CD8 compartments difficult to assess. In a study by Yang et al., $CD4^{-/-}$ mice had a significantly decreased infarct size compared to control mice implicating $CD4^+$ cells in the injury. Interestingly they also showed that CD8 deficiency was not protective and did not change the infarct size (42). Similarly, Burne et al., also showed an insignificant role of $CD8^+$ cells in renal IRI (44). Hence our study proposes $CD8^+$ cells as new players in IRI of the steatotic liver, which thus far had not been considered key mediators of IRI.

With the implication of $CD8^+$ cells in a steatotic liver IRI, we wanted to investigate the underlying mechanism of recruitment of the $CD8^+$ cells into the liver. Adhesion molecules, particularly the selectin family, are involved in homing and recruitment of the lymphocytes in IRI (13, 48). They have also been implicated as mediators of injury in several disease states (12, 40, 44, 46). Studies have shown that blockade of L-selectin attenuates injury after IRI in the kidney (21) and the heart (23). Martinez-Mier et al., showed that anti L-selectin treatment improved liver function and decreased chemokine response (22). This study however alluded to the role of L-selectin in recruiting neutrophils and not $CD8^+$ cells as in our study. Importantly, this study was conducted in lean mice and not in a HFD fed steatotic mouse model.

The findings of our study provide new insight into the mechanisms by which steatosis increases liver damage from IRI. These observations are important in light of the increasing incidence of fatty liver disease, which is making a greater proportion of livers unavailable for transplantation. We show in mice that fatty liver is more highly damaged by ischemia–reperfusion than lean liver; and we identify $CD8^+$ cells as an important cell extrinsic component mediating this damage. Blocking of CD8+ cells, whether by preventing trafficking or by depleting protects against liver injury. These findings might be applied to make steatotic livers from patients who suffer from NAFLD available for transplantation, which would be an important advance due to the increasing shortage of lean donor livers. Decreasing the effects of IRI in a steatotic donor liver might not only make it usable (49), but it could improve outcomes of patients who receive marginal-steatotic livers (33). Furthermore, a large proportion of patients undergoing hepatectomies, myocardial infarction and shock have fatty livers, which respond poorly with delayed recovery (25, 28, 30, 32). Our findings show that these patients are likely to have more severe liver damage than patients with lean livers, and provide strategies for reducing this damage. Though these results need to be verified in different strains of mice and NASH models, we propose that strategies to block L-selectin–mediated homing of $CD8^+$ cells to the fatty liver might reduce the damage caused by ischemia and reperfusion.

Another exciting area of opportunity is the demonstration of acquisition of MECA-79 positive endothelial cells of the liver sinusoidal cells. These needs to be further investigated because they might have a role in immune-mediated liver disease and provide new strategies for therapeutic intervention.

Supplementary Material

Refer to Web version on PubMed Central for supplementary material.

Acknowledgments

We would like to thank Dr. Neil Anthony for assistance with 3D image analysis and Dr. Suresh Venkateswaran for generation of heat maps.

Financial Support:

This work was supported by a K08 grant DK091506 from NIH (NG).

Bibliography

1. Flegal KM, Carroll MD, Kit BK, Ogden CL. Prevalence of obesity and trends in the distribution of body mass index among US adults, 1999–2010. JAMA. 2012; 307:491–497. [PubMed: 22253363]
2. Ogden CL, Carroll MD, Kit BK, Flegal KM. Prevalence of obesity and trends in body mass index among US children and adolescents, 1999–2010. JAMA. 2012; 307:483–490. [PubMed: 22253364]
3. Schiller JS, Lucas JW, Ward BW, Peregoy JA. Summary health statistics for U.S. adults: National Health Interview Survey, 2010. Vital Health Stat. 2012; 10:1–207.
4. Satapathy SK, Sanyal AJ. Epidemiology and Natural History of Nonalcoholic Fatty Liver Disease. Semin Liver Dis. 2015; 35:221–235. [PubMed: 26378640]
5. Feldstein AE, Charatcharoenwitthaya P, Treeprasertsuk S, Benson JT, Enders FB, Angulo P. The natural history of nonalcoholic fatty liver disease in children: A follow-up study for up to 20-years. Gut. 2009
6. Younossi ZM, Stepanova M, Afendy M, Fang Y, Younossi Y, Mir H, Srishord M. Changes in the prevalence of the most common causes of chronic liver diseases in the United States from 1988 to 2008. Clin Gastroenterol Hepatol. 2011; 9:524–530. e521; quiz e560. [PubMed: 21440669]
7. Gupta NA, Kolachala VL, Jiang R, Abramowsky C, Romero R, Fifadara N, Anania F, et al. The glucagon-like peptide-1 receptor agonist Exendin 4 has a protective role in ischemic injury of lean and steatotic liver by inhibiting cell death and stimulating lipolysis. Am J Pathol. 2012; 181:1693–1701. [PubMed: 22960075]
8. Gupta NA, Kolachala VL, Jiang R, Abramowsky C, Shenoi A, Kosters A, Pavuluri H, et al. Mitigation of autophagy ameliorates hepatocellular damage following ischemia reperfusion injury in murine steatotic liver. Am J Physiol Gastrointest Liver Physiol. 2014
9. Caldwell CC, Tschoep J, Lentsch AB. Lymphocyte function during hepatic ischemia/reperfusion injury. J Leukoc Biol. 2007; 82:457–464. [PubMed: 17470532]
10. Zwacka RM, Zhang Y, Halldorson J, Schlossberg H, Dudus L, Engelhardt JF. CD4(+) T-lymphocytes mediate ischemia/reperfusion-induced inflammatory responses in mouse liver. The Journal of clinical investigation. 1997; 100:279–289. [PubMed: 9218504]
11. Huang Y, Rabb H, Womer KL. Ischemia-reperfusion and immediate T cell responses. Cellular immunology. 2007; 248:4–11. [PubMed: 17942086]
12. Chamoun F, Burne M, O'Donnell M, Rabb H. Pathophysiologic role of selectins and their ligands in ischemia reperfusion injury. Frontiers in bioscience : a journal and virtual library. 2000; 5:E103–109. [PubMed: 11056080]
13. Patel KD, Cuvelier SL, Wiehler S. Selectins: critical mediators of leukocyte recruitment. Semin Immunol. 2002; 14:73–81. [PubMed: 11978079]
14. Wedepohl S, Beceren-Braun F, Riese S, Buscher K, Enders S, Bernhard G, Kilian K, et al. L-selectin--a dynamic regulator of leukocyte migration. Eur J Cell Biol. 2012; 91:257–264. [PubMed: 21546114]
15. Gallatin WM, Weissman IL, Butcher EC. A cell-surface molecule involved in organ-specific homing of lymphocytes. Nature. 1983; 304:30–34. [PubMed: 6866086]

16. Schwab N, Schneider-Hohendorf T, Posevitz V, Breuer J, Gobel K, Windhagen S, Brochet B, et al. L-selectin is a possible biomarker for individual PML risk in natalizumab-treated MS patients. Neurology. 2013; 81:865–871. [PubMed: 23925765]
17. Oishi K, Hamaguchi Y, Matsushita T, Hasegawa M, Okiyama N, Dernedde J, Weinhart M, et al. A crucial role of L-selectin in C protein-induced experimental polymyositis in mice. Arthritis Rheumatol. 2014; 66:1864–1871. [PubMed: 24644046]
18. Mitsui A, Tada Y, Shibata S, Kamata M, Hau C, Asahina A, Sato S. Deficiency of both L-selectin and ICAM-1 exacerbates imiquimod-induced psoriasis-like skin inflammation through increased infiltration of antigen presenting cells. Clin Immunol. 2015; 157:43–55. [PubMed: 25572533]
19. Lawson JA, Burns AR, Farhood A, Lynn Bajt M, Collins RG, Smith CW, Jaeschke H. Pathophysiologic importance of E- and L-selectin for neutrophil-induced liver injury during endotoxemia in mice. Hepatology (Baltimore, Md.). 2000; 32:990–998.
20. Toledo-Pereyra LH, Lopez-Neblina F, Lentsch AB, Anaya-Prado R, Romano SJ, Ward PA. Selectin inhibition modulates NF-kappa B and AP-1 signaling after liver ischemia/reperfusion. J Invest Surg. 2006; 19:313–322. [PubMed: 16966210]
21. Rabb H, Ramirez G, Saba SR, Reynolds D, Xu J, Flavell R, Antonia S. Renal ischemic-reperfusion injury in L-selectin-deficient mice. The American journal of physiology. 1996; 271:F408–413. [PubMed: 8770173]
22. Martinez-Mier G, Toledo-Pereyra LH, McDuffie E, Warner RL, Ward PA. L-Selectin and chemokine response after liver ischemia and reperfusion. J Surg Res. 2000; 93:156–162. [PubMed: 10945958]
23. Carter YM, Thomas R, Bargatze R, Jutila M, Murry C, Allen MD. Intracoronary E- and L-selectin blockade attenuates myocardial neutrophil infiltration in cardiac ischemia/reperfusion injury. Curr Surg. 2000; 57:639–640.
24. Galluzzi L, Vitale I, Abrams JM, Alnemri ES, Baehrecke EH, Blagosklonny MV, Dawson TM, et al. Molecular definitions of cell death subroutines: recommendations of the Nomenclature Committee on Cell Death 2012. Cell Death Differ. 2012; 19:107–120. [PubMed: 21760595]
25. Birsner JH, Wan C, Cheng G, Evans ZP, Polito CC, Fiorini RN, Gilbert G, et al. Steatotic liver transplantation in the mouse: a model of primary nonfunction. J Surg Res. 2004; 120:97–101. [PubMed: 15172195]
26. Chavin KD, Fiorini RN, Shafizadeh S, Cheng G, Wan C, Evans Z, Rodwell D, et al. Fatty acid synthase blockade protects steatotic livers from warm ischemia reperfusion injury and transplantation. Am J Transplant. 2004; 4:1440–1447. [PubMed: 15307831]
27. Fiorini RN, Shafizadeh SF, Polito C, Rodwell DW, Cheng G, Evans Z, Wan C, et al. Anti-endotoxin monoclonal antibodies are protective against hepatic ischemia/reperfusion injury in steatotic mice. Am J Transplant. 2004; 4:1567–1573. [PubMed: 15367211]
28. Gomez D, Malik HZ, Bonney GK, Wong V, Toogood GJ, Lodge JP, Prasad KR. Steatosis predicts postoperative morbidity following hepatic resection for colorectal metastasis. Br J Surg. 2007; 94:1395–1402. [PubMed: 17607707]
29. Clavien PA. Selzner MCONLTM, Pmid. Hepatic steatosis and transplantation. Liver transplantation : official publication of the American Association for the Study of Liver Diseases and the International Liver Transplantation Society. 2002; 8:980.
30. Vetelainen R, van Vliet A, Gouma DJ, van Gulik TM. Steatosis as a risk factor in liver surgery. Ann Surg. 2007; 245:20–30. [PubMed: 17197961]
31. Vetelainen R, van Vliet AK, van Gulik TM. Severe steatosis increases hepatocellular injury and impairs liver regeneration in a rat model of partial hepatectomy. Ann Surg. 2007; 245:44–50. [PubMed: 17197964]
32. Matheson PJ, Hurt RT, Franklin GA, McClain CJ, Garrison RN. Obesity-induced hepatic hypoperfusion primes for hepatic dysfunction after resuscitated hemorrhagic shock. Surgery. 2009; 146:739–747. discussion 747-738. [PubMed: 19789034]
33. Selzner M, Clavien PA. Fatty liver in liver transplantation and surgery. Seminars in liver disease. 2001; 21:105–113. [PubMed: 11296690]

34. Charlton MR, Burns JM, Pedersen RA, Watt KD, Heimbach JK, Dierkhising RA. Frequency and outcomes of liver transplantation for nonalcoholic steatohepatitis in the United States. Gastroenterology. 2011; 141:1249–1253. [PubMed: 21726509]
35. Kolachala VL, Jiang R, Abramowsky CR, Gupta NA. Contrast-Based Real-Time Assessment of Microcirculatory Changes in a Fatty Liver After Ischemia Reperfusion Injury. J Pediatr Gastroenterol Nutr. 2016; 62:429–436. [PubMed: 26485605]
36. Seifalian AM, Piasecki C, Agarwal A, Davidson BR. The effect of graded steatosis on flow in the hepatic parenchymal microcirculation. Transplantation. 1999; 68:780–784. [PubMed: 10515377]
37. Ijaz S, Yang W, Winslet MC, Seifalian AM. Impairment of hepatic microcirculation in fatty liver. Microcirculation (New York, N.Y. : 1994). 2003; 10:447–456.
38. Farrell GC, Teoh NC, McCuskey RS. Hepatic microcirculation in fatty liver disease. Anatomical record (Hoboken, N.J. : 2007). 2008; 291:684–692.
39. Selzner M, Rudiger HA, Sindram D, Madden J, Clavien PA. Mechanisms of ischemic injury are different in the steatotic and normal rat liver. Hepatology (Baltimore, Md.). 2000; 32:1280–1288.
40. Geudens N, Vanaudenaerde BM, Neyrinck AP, Van De Wauwer C, Vos R, Verleden GM, Verbeken E, et al. The importance of lymphocytes in lung ischemia-reperfusion injury. Transplant Proc. 2007; 39:2659–2662. [PubMed: 17954201]
41. Yilmaz G, Arumugam TV, Stokes KY, Granger DN. Role of T lymphocytes and interferon-gamma in ischemic stroke. Circulation. 2006; 113:2105–2112. [PubMed: 16636173]
42. Yang Z, Day YJ, Toufektsian MC, Xu Y, Ramos SI, Marshall MA, French BA, et al. Myocardial infarct-sparing effect of adenosine A2A receptor activation is due to its action on CD4+ T lymphocytes. Circulation. 2006; 114:2056–2064. [PubMed: 17060376]
43. Shigematsu T, Wolf RE, Granger DN. T-lymphocytes modulate the microvascular and inflammatory responses to intestinal ischemia-reperfusion. Microcirculation. 2002; 9:99–109. [PubMed: 11932777]
44. Burne MJ, Daniels F, El Ghandour A, Mauiyyedi S, Colvin RB, O'Donnell MP, Rabb H. Identification of the CD4(+) T cell as a major pathogenic factor in ischemic acute renal failure. The Journal of clinical investigation. 2001; 108:1283–1290. [PubMed: 11696572]
45. Kuboki S, Sakai N, Tschop J, Edwards MJ, Lentsch AB, Caldwell CC. Distinct contributions of CD4+ T cell subsets in hepatic ischemia/reperfusion injury. Am J Physiol Gastrointest Liver Physiol. 2009; 296:G1054–1059. [PubMed: 19264952]
46. Khandoga A, Hanschen M, Kessler JS, Krombach F. CD4+ T cells contribute to postischemic liver injury in mice by interacting with sinusoidal endothelium and platelets. Hepatology. 2006; 43:306–315. [PubMed: 16440342]
47. Rabb H, Daniels F, O'Donnell M, Haq M, Saba SR, Keane W, Tang WW. Pathophysiological role of T lymphocytes in renal ischemia-reperfusion injury in mice. American journal of physiology. Renal physiology. 2000; 279:F525–531. [PubMed: 10966932]
48. Springer TA. Traffic signals for lymphocyte recirculation and leukocyte emigration: the multistep paradigm. Cell. 1994; 76:301–314. [PubMed: 7507411]
49. El-Badry AM, Moritz W, Contaldo C, Tian Y, Graf R, Clavien PA. Prevention of reperfusion injury and microcirculatory failure in macrosteatotic mouse liver by omega-3 fatty acids. Hepatology. 2007; 45:855–863. [PubMed: 17393510]

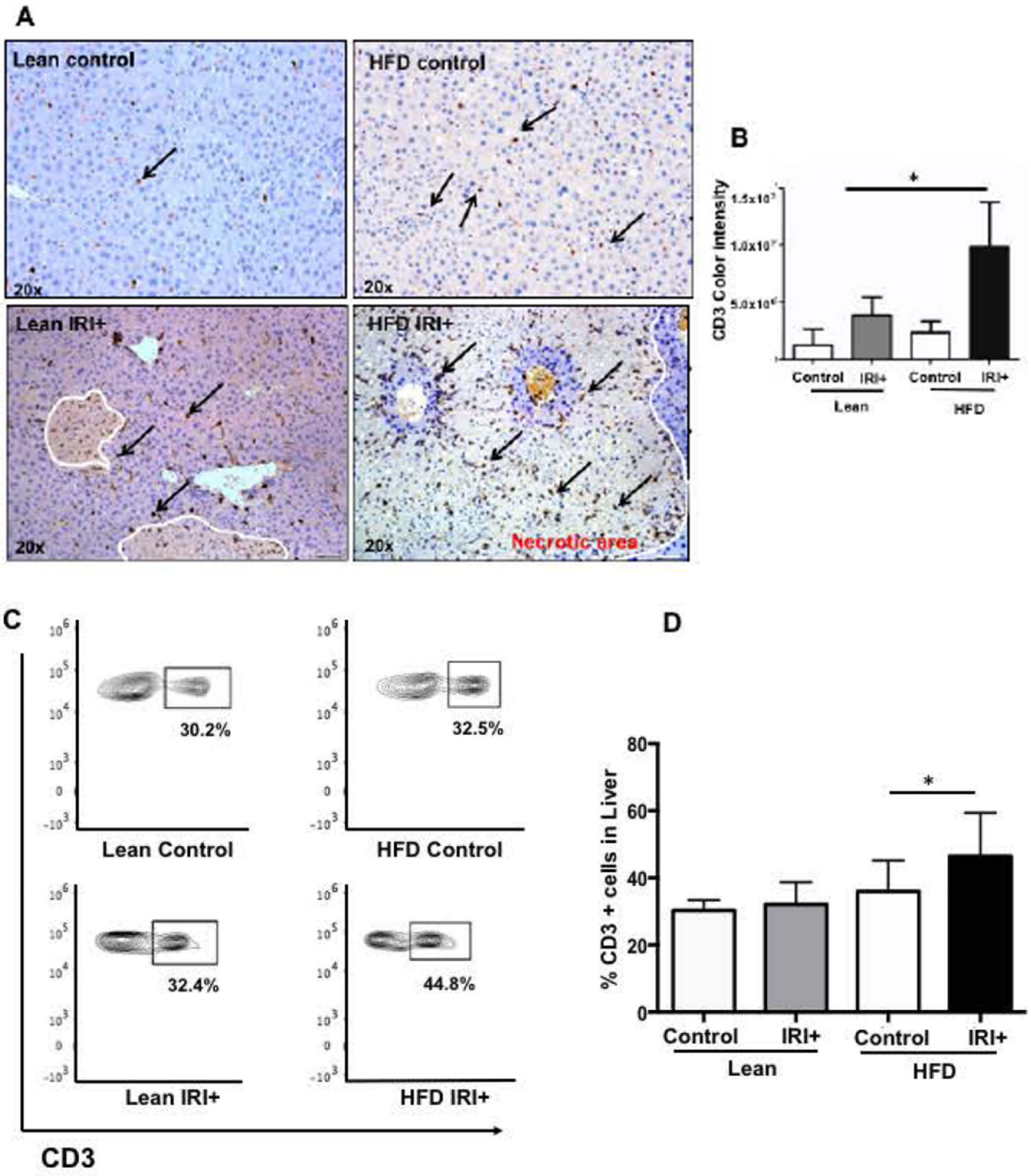

FIG. 1. High Fat Diet (HFD) fed mice have increased hepatocellular injury and number of intrahepatic CD3$^+$ cells after IRI

(A) Immunohistochemical analysis of liver tissues using an antibody against CD3. Representative images are shown, $CD3^+$ cells (brown) in livers from lean and HFD controls (Top panel) and IRI+ (bottom panel) **(B)** $CD3^+$ quantification. **(C)** Flow cytometry of $CD3^+$ cells in livers from lean and HFD control (top panel), with IRI+ (bottom panel) **(D)** graphical representation of percent $CD3^+$ cells from hepatic lymphocytes with quantification. Data represents mean ± SEM of at least 10 mice in each group of 3 independent experiments ($p<0.0001$, Two-way Anova).

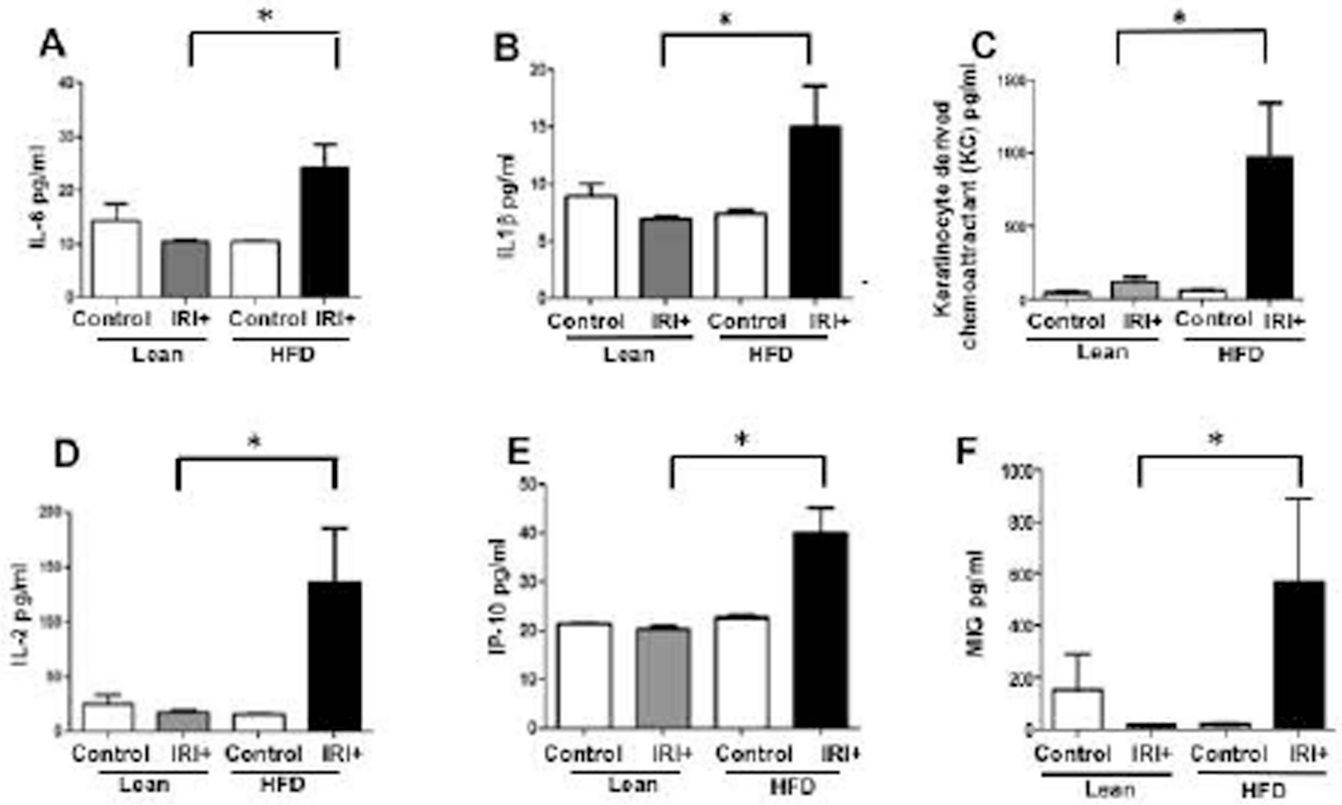

FIG. 2. Increased serum levels of pro-inflammatory cytokines in HFD fed mice after IRI

Pro-inflammatory cytokines analyzed in serum samples from lean and HFD fed mice with and without IRI, demonstrated significantly increased levels in HFD IRI+ Graphical representation of levels of **(A)** IL-6, **(B)** IL-1β, **(C)** keratinocyte-derived chemoattractant, **(D)** IL-2, **(E)** IP-10, and **(F)** MIG are shown. Data represents mean ± SEM of at least 10 mice in each group of 3 independent experiments. Asterisks indicates $p<0.05$, Two-way Anova).

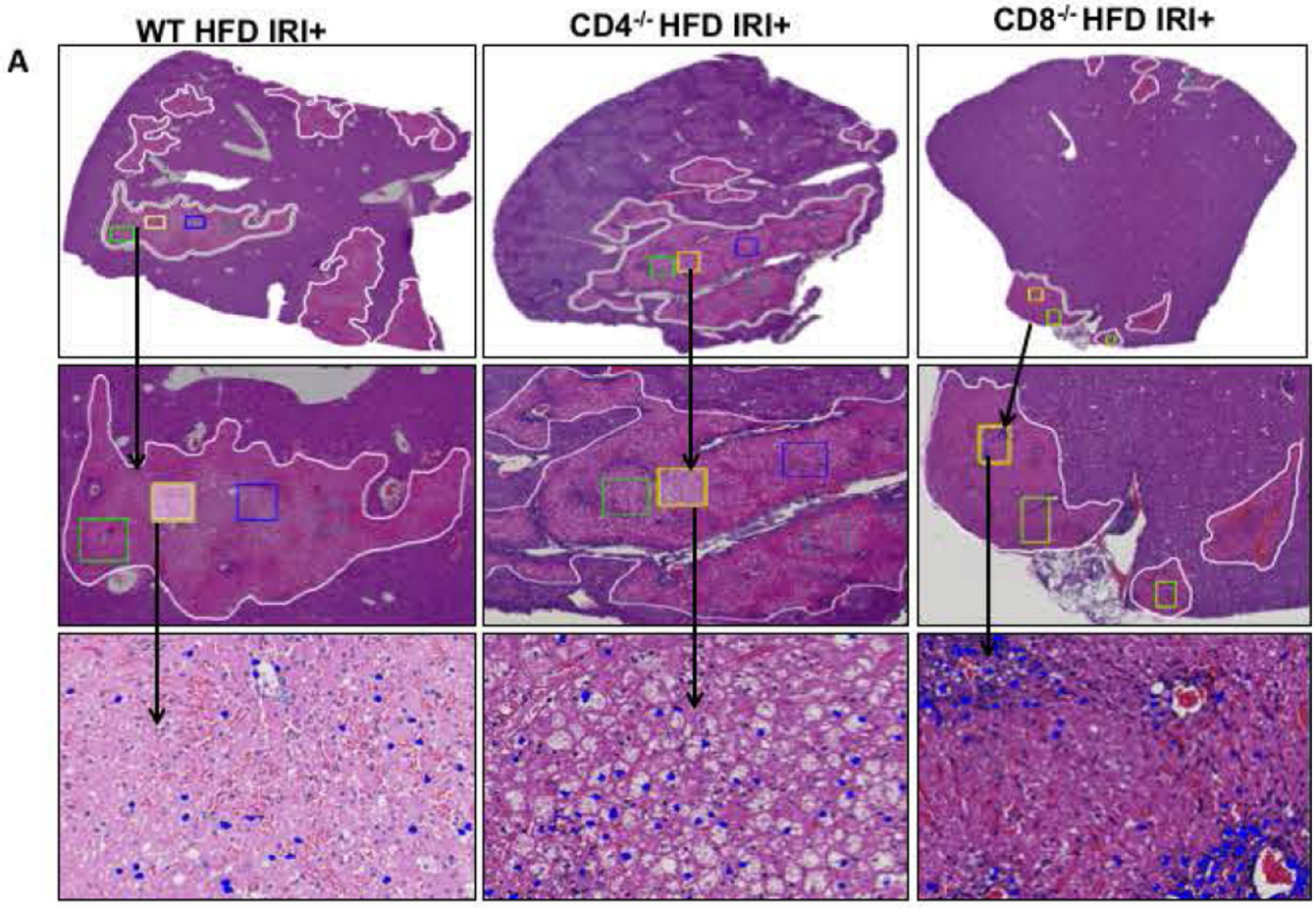

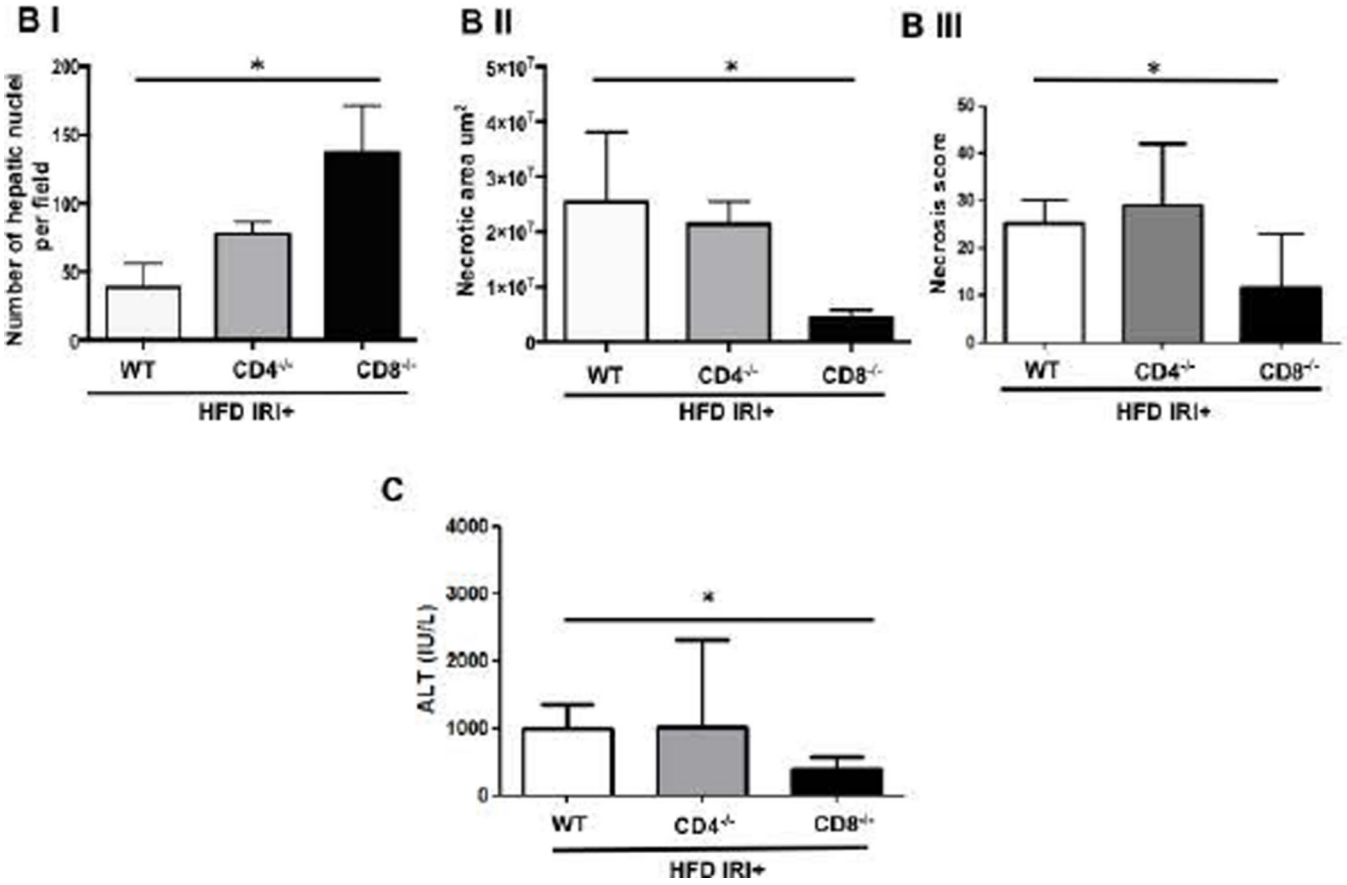

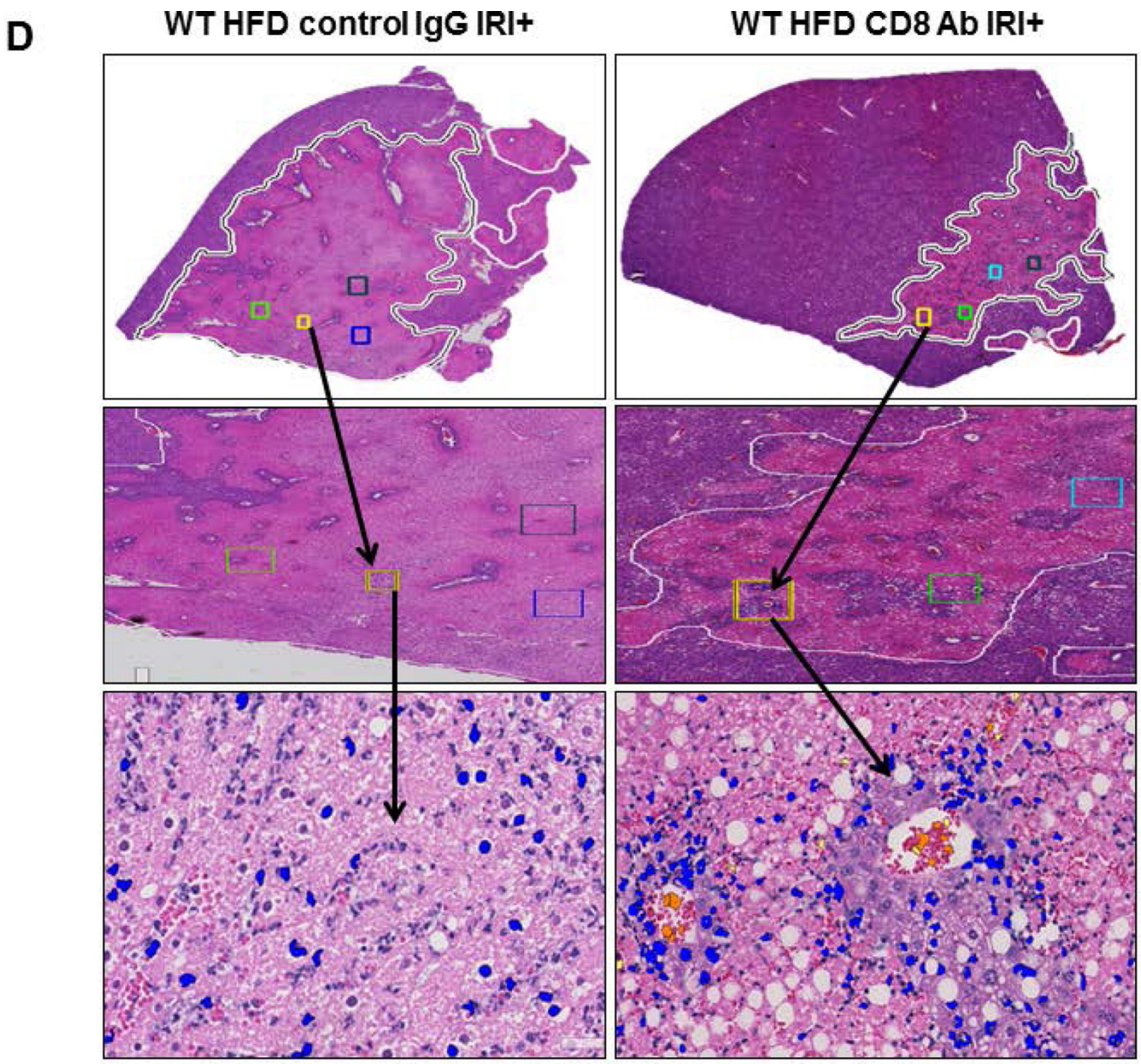

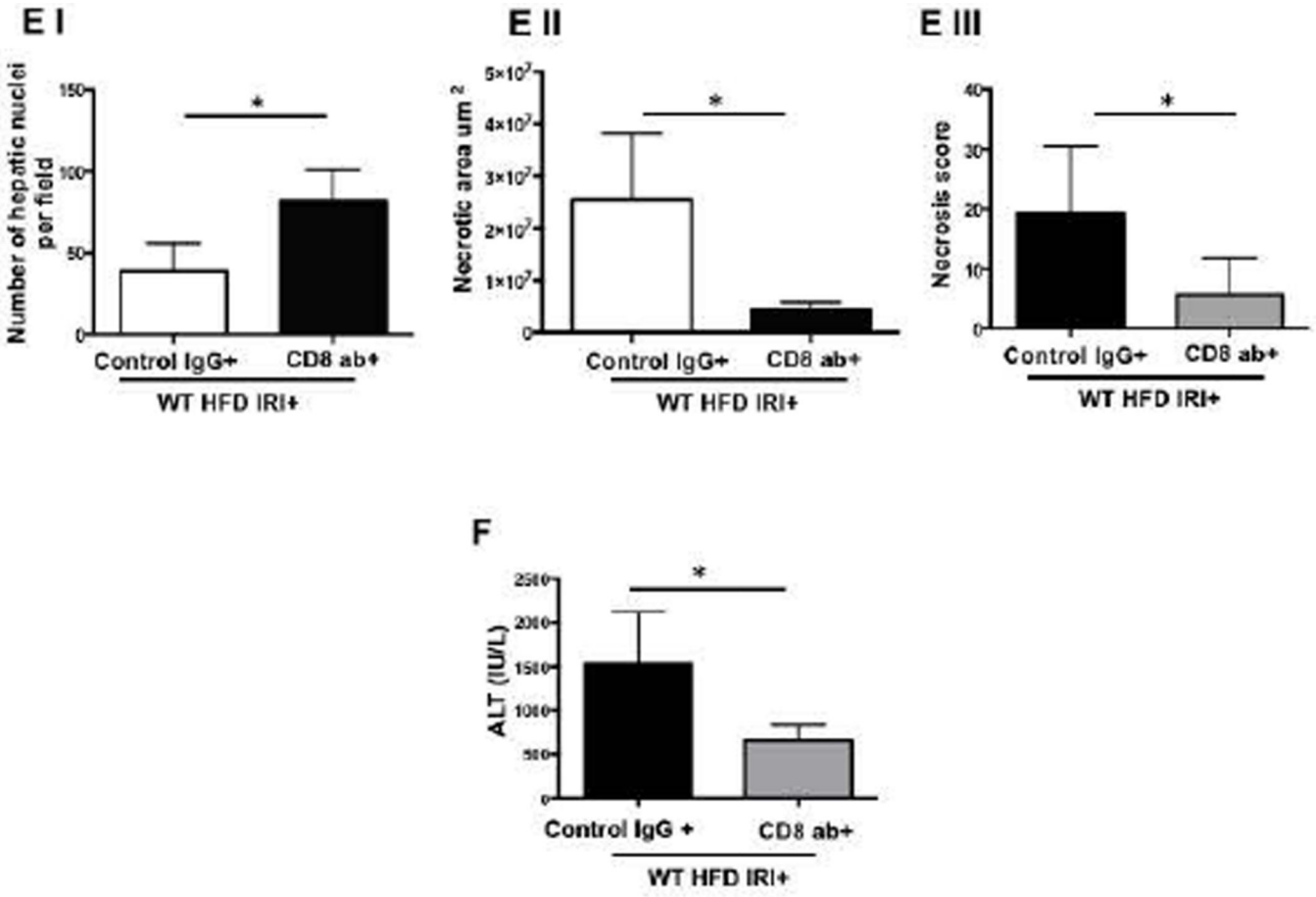

FIG. 3. Loss of CD8, but not CD4 T cells, protects against Ischemia reperfusion injury in HFD fed mice

Histological representation of ischemic liver lobes obtained from HFD fed $CD4^{-/-}$ and $CD8^{-/-}$ mice subjected to IRI. Entire liver lobe undergoing IRI was scanned and representative H&E images demonstrating area of necrosis (outlined by white lines) are shown here. **(A)** Middle panels represent magnified images of top panels respectively and bottom panels represent hepatic nuclei (blue). **(BI, II)** WT vs. $CD8^{-/-}$ for hepatic nuclei per field ($p<0.0001$) and necrotic area ($p<0.02$) **(BIII)** Necrosis score: WT vs. $CD8^{-/-}$ $p<0.01$ (C) ALT: WT vs. $CD8^{-/-}$ $p<0.04$). **(D)** WT HFD fed mice were treated with CD8 depleting antibody and control IgG and subjected to IRI. Panels are represented as described in 3A. **(E)** Graphical representation of Control IgG vs. CD8 Ab for hepatic nuclei ($p<0.001$), necrotic area ($p<0.04$) and necrosis score ($p<0.002$). **(F)** Serum ALT, $p<0.05$. Data represents mean ± SEM of at least 5 mice in each group of 2 independent experiments. Asterisks indicates $p<0.05$, One-way Anova.

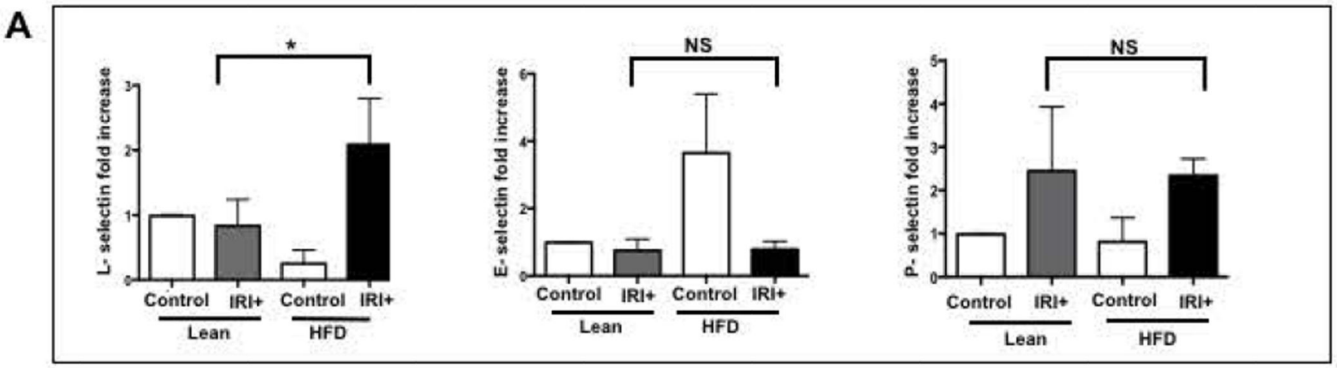

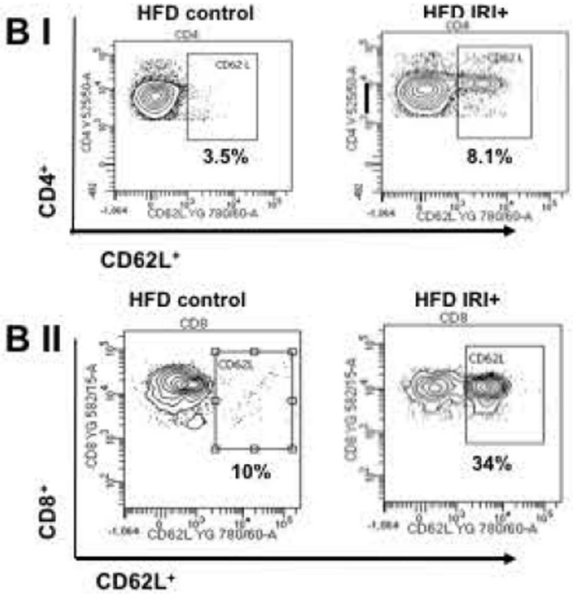

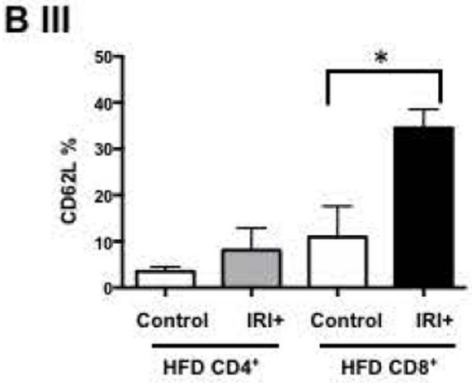

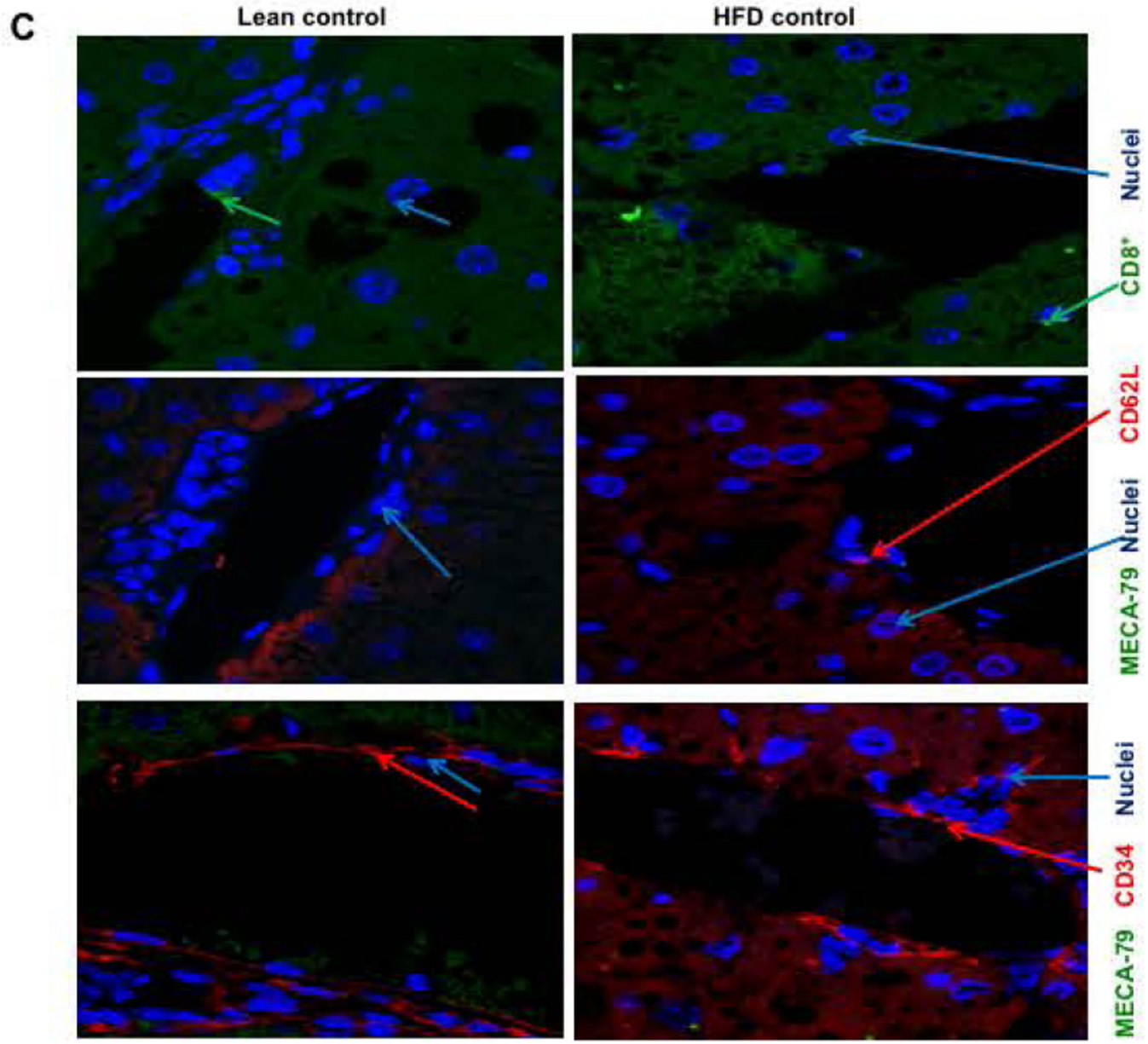

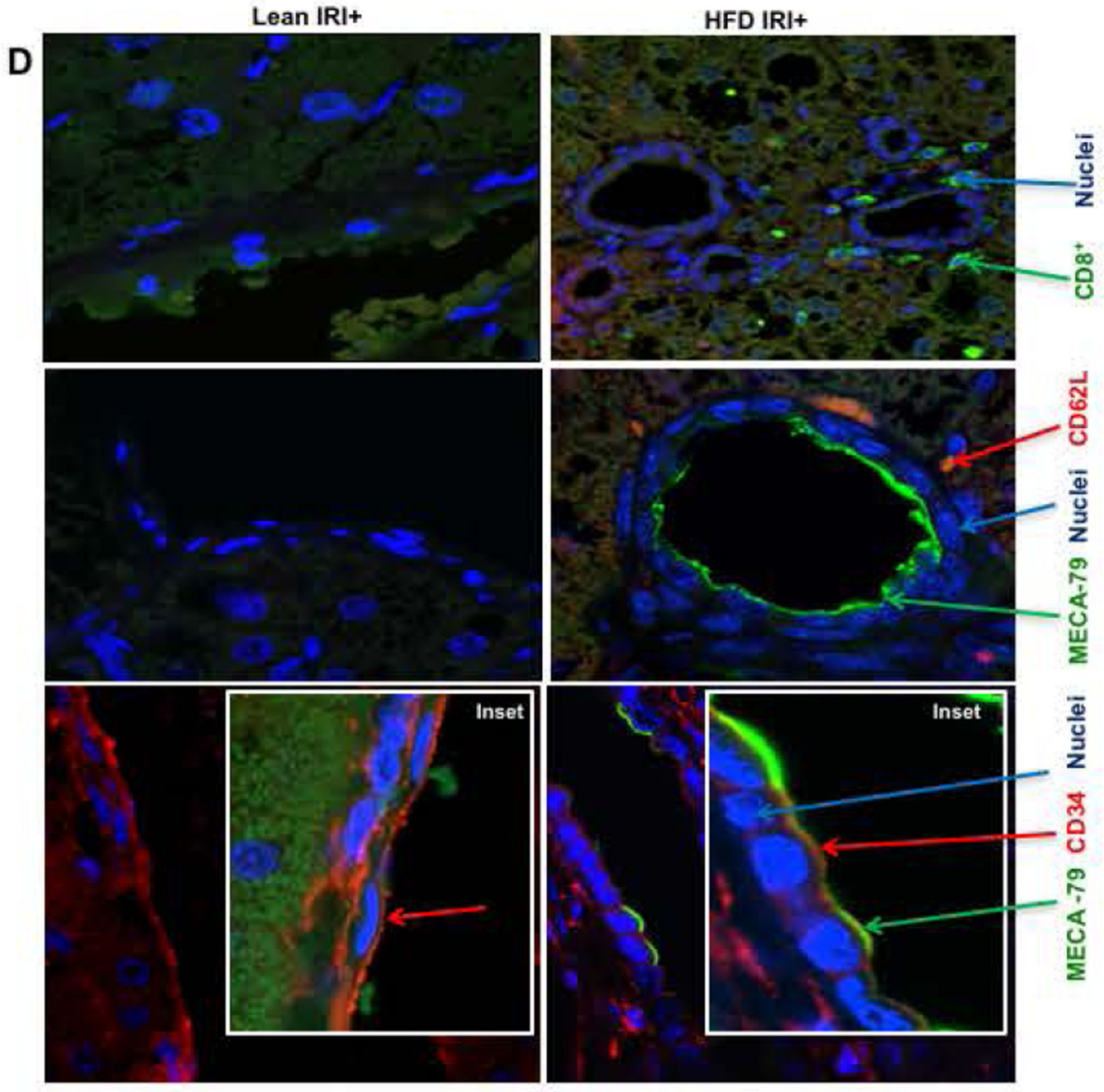

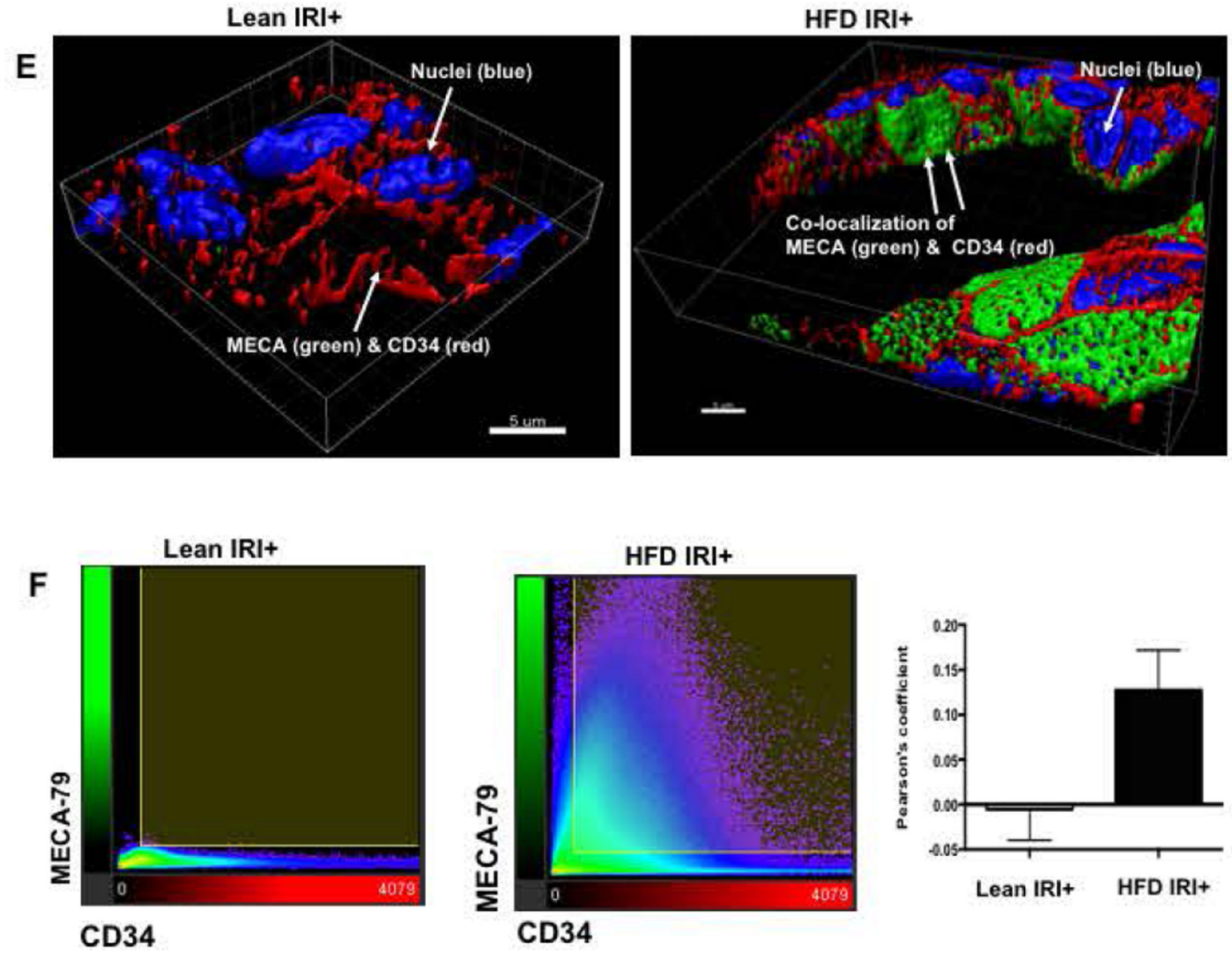

FIG. 4. CD8$^+$ cells mediate IRI induced hepatocellular injury in steatotic liver in HFD fed mice via L-selectin

(A) Real time PCR was performed in total RNA isolated from liver tissues from lean and HFD fed mice undergoing IRI. mRNA levels of L, E and P selectins are graphically represented (L-selectin Lean IRI+ vs. HFD IRI+: $p<0.003$), top panel) **(BI)**. Flow cytometry analyses showing lymphocytes isolated from lean and HFD control and IRI+ which were CD4$^+$/CD62L$^+$ and **(BII)** CD8$^+$/CD62L$^+$ **(BIII)** Graphical representation of number of CD4$^+$ and CD8$^+$ cells that are CD62L$^+$ are shown. CD8$^+$ CD62L$^+$ cells are significantly increased upon IRI exposure in HFD mice compared to HFD controls ($p<0.0002$). **(C, D)** Show representative images from immunofluorescence of CD8$^+$ cells (green) (top panel), co-localization of CD62L (red) and ligand MECA-79 (green) (middle panel) and co-localization of MECA-79 (green) and endothelial cell marker CD34 (red). **(E)**: Co-localization 3D images of CD34 (red) and MECA-79 (green). **(F):** Co-localization quantification is shown by histogram and bar graph. Data represents mean ± SEM of at least 10 mice in each group of 3 independent experiments. Asterisks indicates $p<0.05$, Two-way Anova.

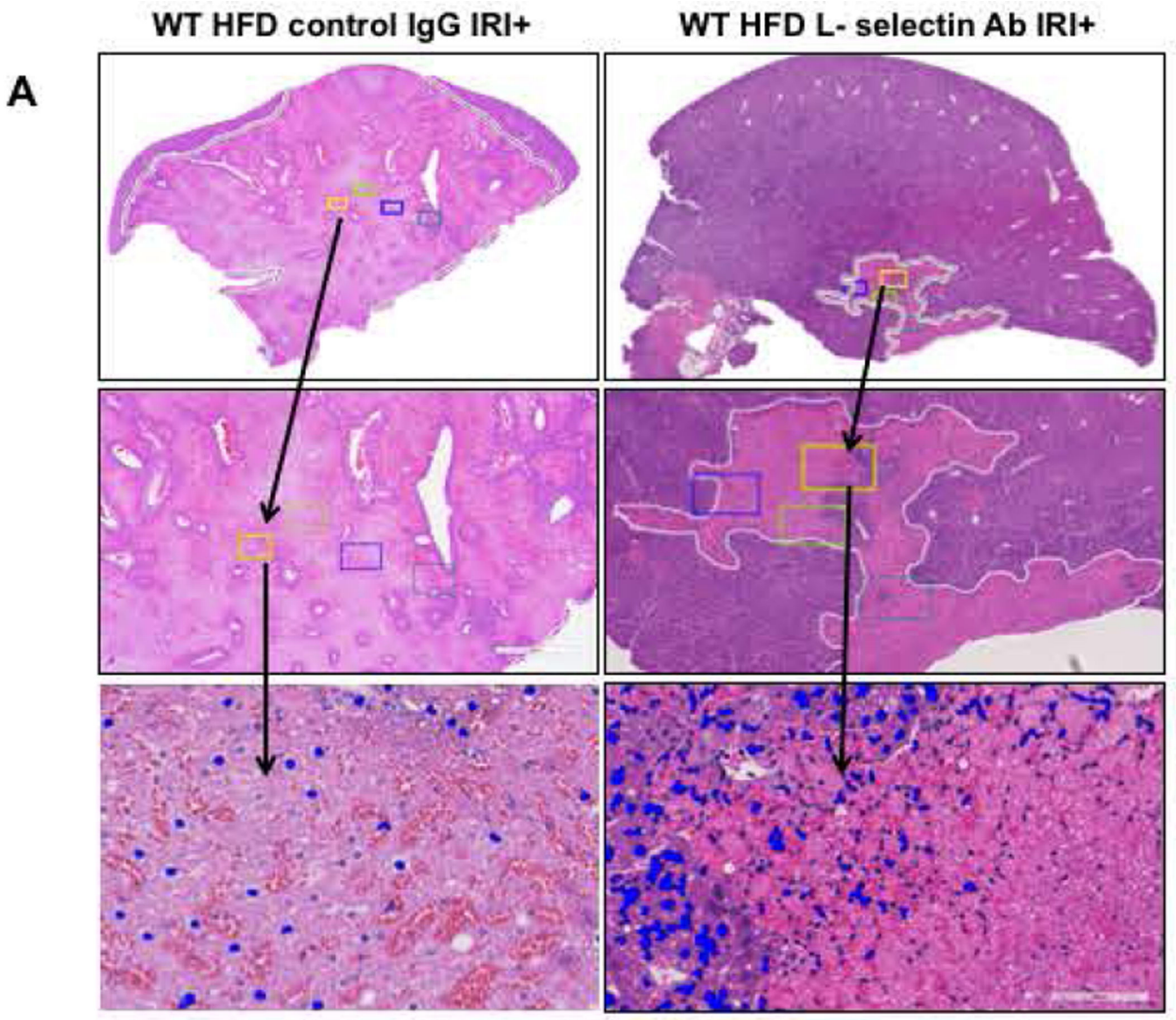

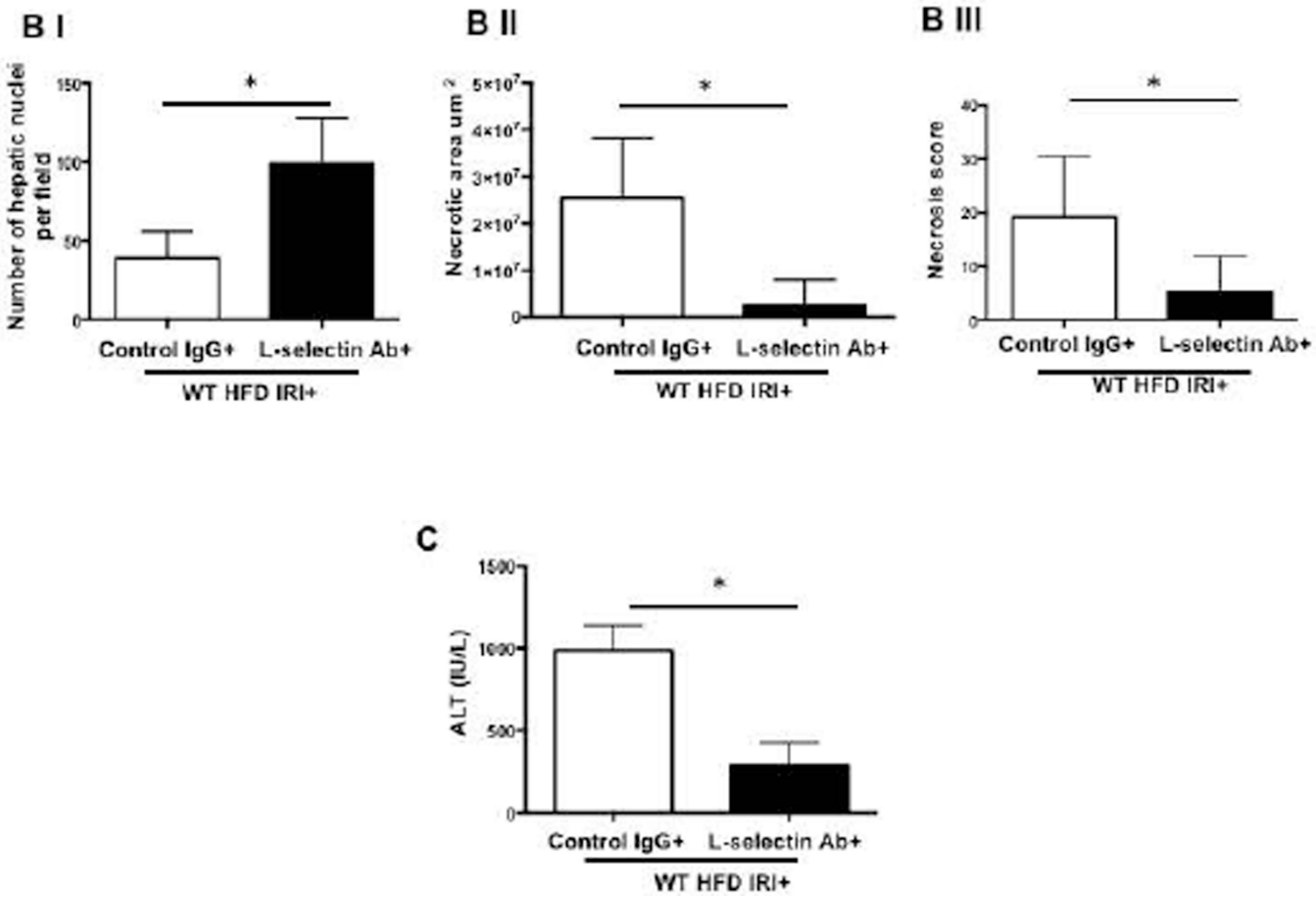

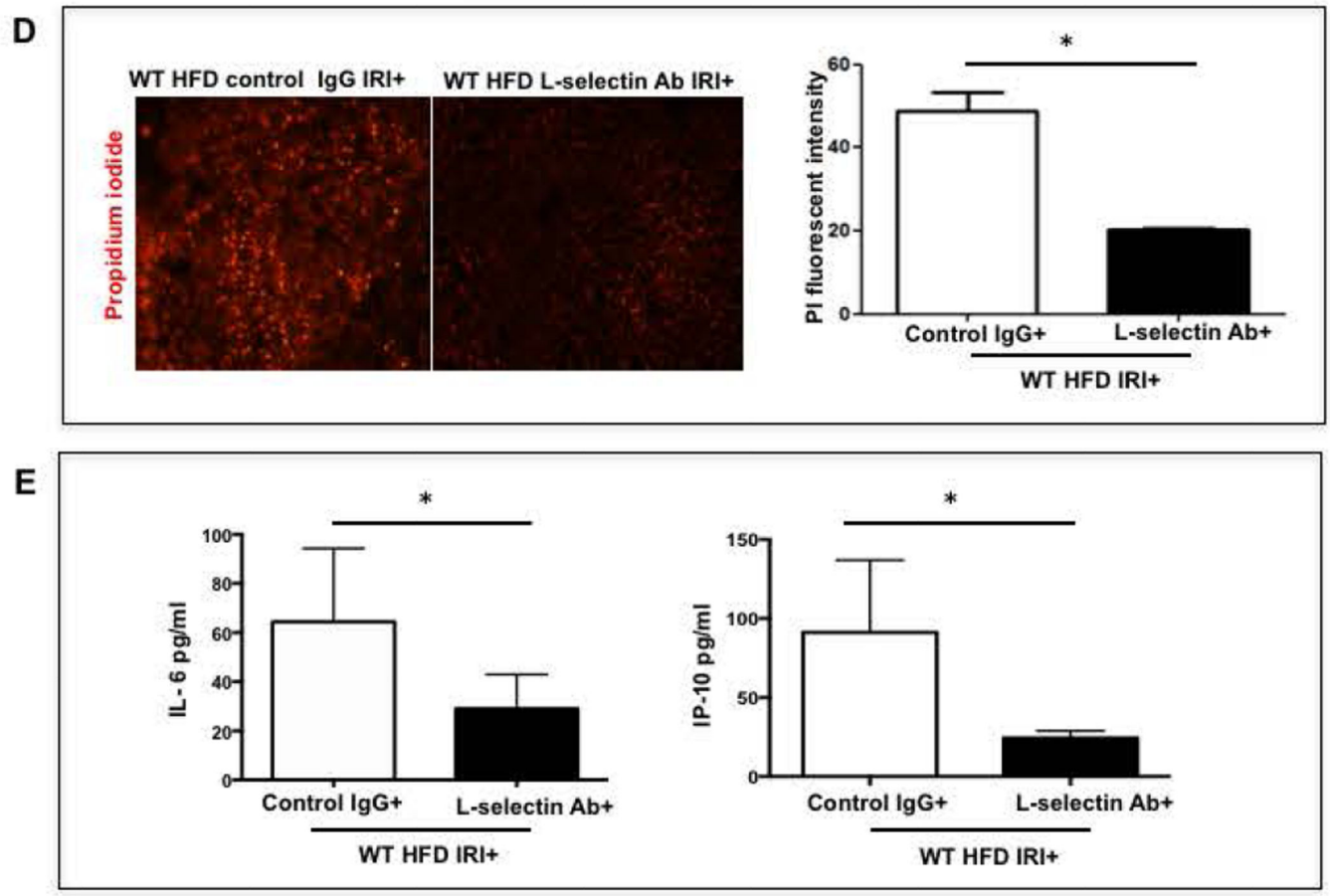

FIG. 5. Blocking L-selectin reduces hepatocellular injury in HFD fed mice after IRI

(A) Histological representation of ischemic liver lobes obtained from WT HFD fed mice treated with control IgG and L-selectin antibody and subjected to IRI. Entire lobe of the liver undergoing IRI was scanned and representative H&E images demonstrating area of necrosis (outlined by white lines) are shown here. Middle panels represent magnified images of top panels and bottom panels represent hepatic nuclei (blue). **(BI,II)** Control IgG vs. L-selectin Ab for hepatic nuclei / field ($p<0.0001$) and necrotic area ($p<0.005$) **(BIII)** Necrosis score ($p<0.002$) (C) ALT ($p<0.004$) **(D)** depicts extent of necrotic cell death by red fluorescent stain, Propidium iodide (PI) positive cells in the liver from HFD IRI+ given control IgG and L-selectin Ab .PI intensity quantification shown on right ($p<0.003$). **(E)** Quantification of serum IL-6 ($p<0.04$) and IP-10 ($p<0.03$) from IgG and L-selectin Ab treated HFD fed mice. Data represents mean ± SEM of at least 10 mice in each group of 3 independent experiments. Asterisks indicates $p<0.05$, student t-test.

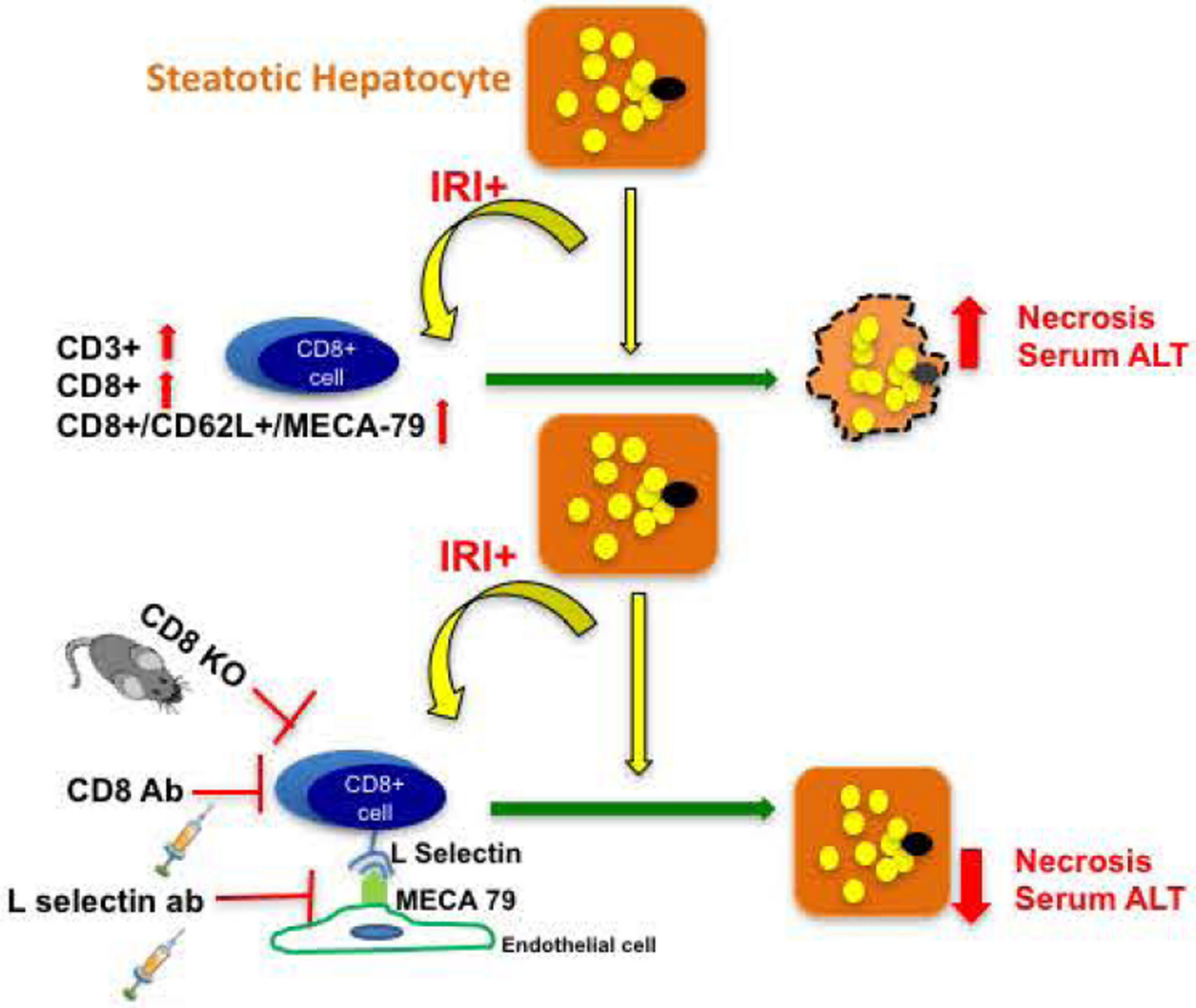

FIG. 6. Schematic representation of proposed mechanism of hepatocyte injury in steatotic liver after IRI

Table 1

Necrosis Scoring

	Score	0	1	2	4
Zone 1					
	Nucleus	Normal	>50 cells	<50 cells	-
	Membrane	Normal	>50 cells	<50 cells	-
	Discernible necrotic tissue	Absent			Present
Zone 2	Nucleus	Normal	>50 cells	<50 cells	-
	Membrane	Normal	>50 cells	<50 cells	-
	Discernible necrotic tissue	Absent			Present
Zone 3	Nucleus	Normal	>50 cells	<50 cells	-
	Membrane	Normal	>50 cells	<50 cells	-
	Discernible necrotic tissue	Absent			Present
Bridging necrosis		Absent	<5	>5	Present
Hemorraghic necrotic tissue		Absent			Present
Total Score					32

Table 2

Primer name	Sequence
L-selectin forward	TGTGGAGCATCTGGAAACTG
L-selectin reverse	AGGAATGAAGAGGGGGTTGT
P-selectin forward	TGCTGTCCATTGTCCTGAAG
P-selectin reverse	CTTTGGTCCGAACACCACTT
E-selectin forward	AGCTACCCATGGAACACGAC
E-selectin reverse	CGTTATCCCAGATGCCAGAT